JOURNAL OF AGRICULTURAL AND FOOD CHEMISTRY

Article

pubs.acs.org/JAFC

Characterization of Trilayer Antimicrobial Diffusion Films (ADFs) Based on Methylcellulose–Polycaprolactone Composites

Afia Boumail,[†] Stephane Salmieri,[†] Emilie Klimas,[†] Pamphile O. Tawema,[†] Jean Bouchard,[‡] and Monique Lacroix*[,†]

[†]INRS-Institute Armand-Frappier, 531 Boulevard des Prairies, Laval, Quebec H7V 1B7, Canada

[‡]FPInnovations, 570 Boulevard St-Jean, Pointe-Claire, Quebec H9R 3J9, Canada

ABSTRACT: Novel trilayer antimicrobial diffusion films (ADFs) were developed for food applications. ADFs were composed of two external layers of polycaprolactone and one internal layer of nanocrystalline cellulose (NCC)-reinforced methylcellulose (MC) matrix. Two antimicrobial mixtures (formulations A and B) were incorporated in the MC layer and compared via the evaluation of film properties. Resulting ADFs were inserted as diffusion devices into vegetable packages, and samples were stored at 4 °C for 14 days. Microbiological diffusion assays in the presence of ADFs were performed on pathogenic bacteria. From this, the study focused on characterizing the structural, physicochemical properties and total phenols (TP) release from ADFs. This TP release was determined by Folin–Ciocalteu's method and by FTIR analysis. Results indicated a controlled release of antimicrobials into the headspace (16.5% for formulation A and 13.4% for formulation B). Good correlations (≥90%) between both methods allowed validating an innovative, accurate, rapid FTIR procedure to quantify the diffusion of TP. SEM micrographs showed fibrillar structure due to NCC and a more compact network due to antimicrobials. Encapsulated antimicrobial formulations induced color changes without affecting visual attributes of films. ADFs containing formulation B exhibited the highest tensile strength (17.3 MPa) over storage.

KEYWORDS: *antimicrobial film, diffusion, methylcellulose, polycaprolactone, nanocrystalline cellulose, composite*

INTRODUCTION

Recently, foodborne microbial outbreaks have generated many research programs for the development of innovative methods to inhibit microbial growth in foods while maintaining quality, freshness, and safety.[1,2] In this context, the addition of functional antimicrobial ingredients in food presents many perspectives, particularly by focusing on (i) the stability of antimicrobial compounds during processing and storage and (ii) the need to prevent undesirable sensorial interactions with the food matrix. Therefore, the encapsulation of antimicrobial ingredients in polymer could help to solve these two concerns.[3,4]

Essential oils (EOs), secondary metabolites of plants, are complex mixtures of volatile substances. They contain large amounts of active compounds such as phenolic acids and flavonoids, which provide strong antimicrobial or antioxidant properties and low toxicity compared with those from synthetic phenolic antioxidants, such as butylated hydroxytoluene (BHT).[5−7] These remarkable properties induce these natural agents to be used as alternative food preservatives.[8] However, due to their high relative volatility and thereby the difficulty to control their release into food products, the use of EOs may not be fully effective when directly applied on food. Their encapsulation in a polymeric matrix such as packaging films, edible coatings, or diffusion films could provide an alternative issue to ensure their stability in such a way that only desired levels of the preservatives diffuse progressively and come into contact with the food.[3,7,9−12] Previous studies showed that the incorporation of essential oils in alginate-based films could provide a reduction of the bacterial load up to 5 days due to the liberation of antimicrobial compounds.[9,10]

Polycaprolactone (PCL) is a semicrystalline biodegradable polyester providing good water resistance and good processability.[13] It can be used to produce biodegradable water-resistant films, is compatible with various polymer blends,[14−16] and therefore provides excellent properties for patch applications in humid environments. Methylcellulose (MC) is a cellulose ether that has been widely used for many years in industry to produce gels and fine chemicals in pharmaceuticals, foods, paints, and cosmetics.[17] Nanocrystalline cellulose (NCC) is another cellulose derivative having particles with a diameter of 2−20 nm and a length of a few hundred nanometers. The network created within the matrix provides mechanical reinforcement into polymer bulk.[18] Some studies have reported that NCC can increase the stability of encapsulated antimicrobial agents into film matrices.[17,19−21]

The aim of the present study was to characterize trilayer antimicrobial diffusion films (ADFs) composed of PCL/MC/PCL. Natural antimicrobial agents (formulations A and B) were incorporated into internal MC-based films. A preliminary antimicrobial assay was performed against *Escherichia coli* O157:H7, *Salmonella* Typhimurium, and *Listeria monocytogenes* to evaluate in vitro antimicrobial properties of ADFs. Films were also introduced in packages containing precut vegetables and stored for 14 days at 4 °C. The molecular structure of ADFs was revealed by Fourier transform infrared (FTIR) spectroscopy, and their cross-section morphology was inves-

Received: October 17, 2012
Revised: December 20, 2012
Accepted: January 3, 2013
Published: January 3, 2013

tigated by scanning electron microscopy (SEM). The total phenolic (TP) volatiles release was evaluated by Folin−Ciocalteu's method and also by FTIR analysis, via semi-quantification of encapsulated antimicrobials, for correlation purposes. Colorimetric parameters and mechanical properties of ADFs were measured to determine their variations over storage.

The innovation of this work consists in the development of trilayer diffusion films containing natural antimicrobials for direct application on vegetables. The second aspect is the determination of the percentage of bioactive compounds released from the films over storage by fast FTIR method.

EXPERIMENTAL PROCEDURES

Materials. *Antimicrobial Formulations.* EO mixtures (formulations A and B) were provided from BSA Ingredients s.e.c./l.p. (Montreal, QC, Canada). Liquid smoke, composed of a mixture of organic acids, was from Kerry Ingredients and Flavours (Monterrey, TN, USA). Rosemary extract was from P. L. Thomas and Co., Inc. (Morristown, NJ, USA).

Film Ingredients. MC (M_n ~ 40000; viscosity = 400 cP, 2% in water at 20 °C) and PCL (M_n ~ 80000) were from Sigma-Aldrich Canada Ltd. (Oakville, ON, Canada). Nanocrystalline cellulose (NCC) was provided by FPInnovations (Pointe Claire, QC, Canada). Glycerol, used as a plasticizer, and Tween 80, as an emulsifier, were purchased from Laboratoire Mat (Beauport, QC, Canada). Vegetable oil (VO) was used as a hydrophobic agent in the film formation process to stabilize hydrophobic compounds via emulsion systems and was bought from a local distributor (Metro, Laval, QC, Canada).

Reagents. Sodium carbonate (monohydrate), Folin−Ciocalteu's phenol reagent, and gallic acid were from Sigma-Aldrich Canada Ltd. (Oakville, ON, Canada).

Methods. *Preparation of PCL Films (External Layers).* PCL compressed films were prepared by compression molding, according to a procedure developed by Sharmin et al.[22]

Preparation of MC-Based Films (Antimicrobial Internal Layer). (a) Preparation of NCC Suspension. A 2% (w/v) NCC aqueous suspension was prepared under stirring before sonication at room temperature for 30 min, using a sonicator bath Branson DHA-1000 (Branson Ultrasonics Corp., Danbury, CT, USA) at a frequency of 40 kHz. Tween 80 was then added under stirring at room temperature.

(b) Dispersion of Antimicrobials in the NCC Suspension. EOs were added to the NCC suspension along with the liquid smoke. Rosemary extract was solubilized in water, at 40 °C under stirring, and then added to the former suspension. The solutions containing the antimicrobial agents were then mixed with the NCC suspension under stirring, for 5 min at room temperature. The resulting antimicrobial suspensions were then homogenized at room temperature, using a digital Ultra-Turrax T25 disperser (IKA Works Inc., Wilmington, NC, USA), at 20000 rpm for 1 min.

(c) Preparation of Antimicrobial MC Matrix. MC was solubilized in distilled water, under stirring at 40 °C (for pregelatinization), and was then cooled in an ice bath to ensure complete solubilization. Then, VO and glycerol were added to the MC suspension, and the mixture was stirred vigorously for 10 min at room temperature. The NCC suspension (containing antimicrobials) was slowly added to the MC suspension, under vigorous stirring. Composite films were cast by applying 15 mL of the film-forming suspension onto Petri dishes (95 × 15 mm; Fisher Scientific, Ottawa, ON, Canada) and allowed to dry (i) for 2 h at 40 °C and (ii) for 24 h at 20 °C. The matrix composition (dry basis) of MC-based films obtained (thickness ~ 25−30 μm) was 46.1 (w/w) MC, 15.4% VO, 23.1% glycerol, 7.7% NCC, and 7.7% Tween 80. Otherwise, for comparison purposes, MC-based films containing formulations A and B were assigned to MC-A and MC-B, respectively, whereas MC-based films containing no antimicrobials were designated MC-control.

Preparation of ADFs as Trilayer Composites PCL/MC/PCL. Trilayer composite films were fabricated similarly to the compression molding process of PCL films described above. This compression molding step was used to form insoluble films. Each internal and external film weighed around 500 mg. Compression molding was operated at 120 °C for 1 min without compression and then with 1 ton pressure for 1 min before cooling for 2 min. PCL/MC/PCL trilayer films (namely, ADF; thickness ~ 225−280 μm) were collected and used immediately for testing. For comparison purposes, ADFs containing formulations A and B were assigned to ADF-A and ADF-B, respectively, whereas ADFs containing no antimicrobial were designated ADF-control.

Evaluation of the Antimicrobial Properties of Films. (a) Preparation of Bacterial Strains. E. coli O157:H7 EDL 933 (INRS-Institut Armand Frappier, Laval, QC, Canada), *Salmonella* Typhimurium SL1344 (INRS-Institut Armand-Frappier), and *L. monocytogenes* 2812 1/2a (Health Canada, St-Hyacinthe, QC, Canada) were maintained at −80 °C in tryptic soy broth (TSB, Difco Laboratories, Detroit, MI, USA) containing 10% glycerol. Prior to the experiment, stock cultures were propagated through two consecutive 24 h growth cycles in TSB at 37 °C to obtain working cultures containing approximately 10^9 CFU/mL.

(b) Antimicrobial Assay of Pathogenic Bacteria. The antimicrobial activity of MC-based films was evaluated according to a modified procedure used by Rojas-Grau et al.[23] Films were cut into 7.5 mm diameter disks and were placed on Mueller−Hinton (Oxoid Ltd., Basingstoke, UK) previously streaked with a solution containing 10^9 CFU/mL bacteria.

Treatments of Vegetables with ADFs. ADFs were inserted into high-barrier packaging bags (Deli One, 3 mil nylon/EvOH/polyethylene, 8 × 10; Winpak Division Ltd., Montreal, QC, Canada) containing vegetable (100 g) and sealed under air. Sealed packages were then stored immediately at 4 °C for physicochemical analysis of films during 14 days of storage.

TP Release of Antimicrobial Compounds. (a) Determination by Spectrophotometry. The availability of total phenols (TP) in ADF-A and ADF-B was determined using Folin−Ciocalteu's procedure, according to a modified method developed by Salmieri and Lacroix.[24]

The concentration of TP was determined according to the equation

$$\text{TP } (\mu\text{g GAE/mg film}) = \frac{((A_{\text{ADF-A or -B}} - A_{\text{ADF-control}}) + b) \times V}{a \times m_{\text{ADF-A or -B}}}$$

where $A_{\text{ADF-A or -B or -control}}$ = absorbance of ADF-A, -B, or -control; V = volume of extract; $m_{\text{ADF-A or -B}}$ = mass of ADF-A or -B extracted; a = slope of the standard curve; and b = Y-intercept of the standard curve.

TP release was deduced from TP availability in film, according to the equation

$$\text{TP release } (\%) = \left(1 - \frac{\text{TP}}{\text{TP}_i}\right) \times 100$$

where TP_i is the initial concentration of TP in films at day 0.

A 2 periods-moving average regression was used to represent the TP release of antimicrobials from ADF-A and -B to smooth out short-term variations and highlight long-term trends over storage, via periodic extrapolation.

(b) Determination by ATR-FTIR Spectroscopy. FTIR spectra of the films were recorded using a Spectrum One spectrophotometer (Perkin-Elmer, Woodbridge, ON, Canada) equipped with an attenuated total reflectance (ATR) device for solids analysis and a high-linearity lithium tantalate (HLLT) detector. Spectra were analyzed using Spectrum 6.3.5 software. Film components, PCL/MC/PCL trilayer films (ADFs), and MC-based films (internal layer) were analyzed for structural characterization and for evaluating the available content of TP in ADFs during storage. Samples were placed onto a zinc selenide crystal, and the analysis was performed within the spectral region of 650−4000 cm^{-1}, with 64 scans recorded at 4 cm^{-1} resolution. After attenuation of total reflectance and baseline correction, spectra were normalized with a limit ordinate of 1.5 absorbance units. Hence, resulting FTIR spectra were compared (i) to identify typical vibration bands related to film components and also (ii) to attribute vibration bands assigned to antimicrobial components

specifically and their respective peak intensities for estimation of the TP release. Peak absorbance was measured for MC-A and MC-B during storage by determining the height of peaks (with MC-control as a blank) with Spectrum software. Finally, data obtained by Folin–Ciocalteu's method and by FTIR were compiled, and mathematical correlations were performed between absorbance of FTIR peaks related to antimicrobial volatiles and TP measurements to validate the feasibility of FTIR analysis to evaluate the TP release of antimicrobial compounds from ADFs.

(c) Scanning Electron Microscopy Analysis (SEM). SEM was used to investigate the effect of NCC and antimicrobial incorporation on the cross-section morphology of MC internal layers. MC layers were prepared for SEM using a freeze fracture technique by allowing a MC piece (5 × 5 mm) to equilibrate under liquid nitrogen. Film samples were held between tweezers and then fractured in liquid nitrogen. Samples were then deposited on an aluminum holder and sputtered with gold–palladium alloy (Au/Pd deposition rate of 30 s equivalent to a coating thickness of 50 Å) in a Hummer IV sputter coater. SEM photographs were taken using a Hitachi S-4700 FEG-SEM (Hitachi Canada Ltd., Mississauga, ON, Canada) at magnifications of 40000× and 100000× at room temperature and a X-ray detector (model 7200, Oxford Instruments, Abingdon, UK) with a resolution of 1.36 eV at 5.9 keV. The working distance was maintained around 8 mm, and the acceleration voltage used was 2 kV.

Physicochemical Properties of Films. (a) Colorimetry of Films. The color of the films was measured using a Colormet with a flat window (Instrumar Engineering Ltd., St. Johns, NF, Canada). Measurements of spectral reflectance were performed directly onto the film surface (viewing area = 10 × 20 mm). The L^*, a^*, b^* system (CIELAB) was employed; the L^* axis represents the lightness from black ($L^* = 0$) to absolute white ($L^* = 100$), the a^* axis varies from green (−) to red (+), and the b^* axis varies from blue (−) to yellow (+). To characterize more precisely the color of ADFs, the hue angle (hue = $\arctan(b^*/a^*)$ if $a^* > 0$ and hue = $\arctan(b^*/a^*) + 180°$ if $a^* < 0$) was determined to indicate color changes between a^* (green color) and the intersection of a^* and b^*, from green (hue = 0°) to yellow color (hue = 90°).

(b) Mechanical Properties of Films. Tensile strength (TS) and tensile modulus (TM) were measured according to the method developed by Khan et al.[17]

Experimental Design and Statistical Analysis. Samples were separated into three groups: (i) ADF-control; (ii) ADF-A; (iii) ADF-B. All measurements were performed in triplicate ($n = 3$). FTIR, TP measurements, and determination of mechanical properties were done using a 2 × 3 × 3 × 7 factorial design: 2 repetitions, 3 replicates, 3 treatments (ADF, ADF-A, ADF-B), and 7 days of storage (0, 1, 2, 6, 8, 10, and 13). SEM was performed at day 0 (day of fabrication) to characterize films after compression molding. Color measurements were realized according to a 3 × 3 × 3 factorial design: 3 replicates, 3 treatments, 3 days of storage (0, 6, and 13). Analysis of variance, Duncan's multiple-range test, and Student t test were performed for statistical analysis by using PASW Statistics 18.0 software (IBM Corp., Somers, NY, USA). Differences between means were considered to be significant at a 5% level.

RESULTS AND DISCUSSION

Antimicrobial Assay. Antibacterial activity of internal films from ADFs is shown in Table 1 and illustrated in Figure 1. MC-control did not inhibit any growth of tested pathogenic bacteria. Notable inhibitory zones were detected for MC-A and -B against *E. coli*, *S.* Typhimurium, and *L. monocytogenes*. Results showed no significant difference ($p > 0.05$) between MC-A and -B for each bacteria (10.7–12.8 mm for MC-A and 11.5–13.6 mm for MC-B), suggesting that both antimicrobial films had similar inhibitory efficiency. Also, MC-A and -B induced similar inhibitory zones against *L. monocytogenes* and *E. coli* ($p > 0.05$), with diameter values around 10.7–10.8 mm for MC-A and 11.5 mm for MC-B. Besides, both films generated significantly larger inhibitory areas ($p \leq 0.05$) against *S.* Typhimurium as compared to other bacteria, with values between 12.8 and 13.6 mm (Figure 1). Such observations of high efficiency of antimicrobials against Gram-negative bacteria were reported by Jin and Zhang[25] and Lopez et al.,[26] in relation with pH and external conditions during storage. Although EOs are generally less efficient against Gram-negative bacteria (due to a more resistant structure of their cell wall membrane), the authors explained such unexpected results by the antimicrobial mechanism generated via the diffusion of volatile compounds and their effectiveness from the film to the package headspace, in relation with the concentration of antimicrobials in the closed atmosphere as a function of time, that is, the difference of diffusion through the polymeric matrix. Oussalah et al.[9] have determined the minimum inhibitory concentrations (MIC) of several EOs on four pathogenic bacteria, showing that the inhibition of bacteria depends on the concentration of EOs. They indicated that the MIC on *L. monocytogenes* and *E. coli* can vary from 2 to 4 times the MIC of *S.* Typhimurium. Those results are consistent with those obtained from the antimicrobial assay.

Table 1. Antibacterial Activity of ADFs against *E. coli*, *L. monocytogenes*, and *S.* Typhimurium

	inhibitory zone (mm) against pathogens[a]		
type of film	*E. coli*	*L. monocytogenes*	*S.* Typhimurium
ADF-control	ND a,A	ND a,A	ND a,A
ADF-A	10.7 ± 0.5 b,A	10.8 ± 0.3 b,A	12.8 ± 1.2 b,B
ADF-B	11.5 ± 0.4 b,A	11.5 ± 0.3 b,A	13.6 ± 1.1 b,B

[a]Means followed by the same lower case letter in each column are not significantly different at the 5% level. Means followed by the same upper case letter in each row are not significantly different at the 5% level. ND, nondetectable (no inhibitory zone detected).

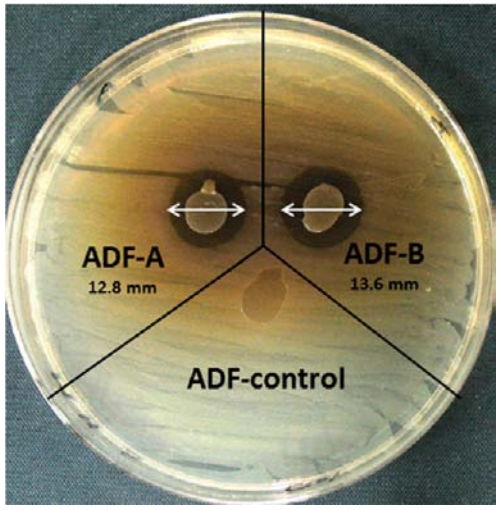

Figure 1. Inhibitory zones of *S.* Typhimurium growth on a bacterial plate induced by trilayer ADF-control, ADF-A, and ADF-B.

TP Release by Spectrophotometry. The availability of TP content of MC-A and MC-B internal layers during storage is presented in Table 2, and their corresponding release is depicted in Figure 2. The profiles of diffusion in Figure 2 were designed mathematically according to a 2 periods-moving average regression to smooth out short-term variations and highlight long-term trends over storage. The moving average model is very useful to estimate the global trend of TP release

Table 2. Determination of Total Phenolic (TP) Content in ADF-A and ADF-B during Storage

	TP concentration[a] (μg GAE/mg film)						
film	day 0	day 1	day 2	day 6	day 8	day 10	day 13s
ADF-A	68.3 ± 4.9 a,E	63.3 ± 5.1 a,D	61.5 ± 4.3 a,D	53.4 ± 5.2 a,B	57.2 ± 4.6 a,C	50.6 ± 7.9 a,A	57.0 ± 4.7 a,C
ADF-B	68.2 ± 4.9 a,D	65.1 ± 6.2 a,C	62.0 ± 5.2 a,B	60.2 ± 4.0 b,AB	62.2 ± 4.7 b,B	58.3 ± 5.2 b,A	59.0 ± 4.5 b,A

[a]Means followed by the same lower case letter in each column are not significantly different at the 5% level. Means followed by the same upper case letter in each row are not significantly different at the 5% level.

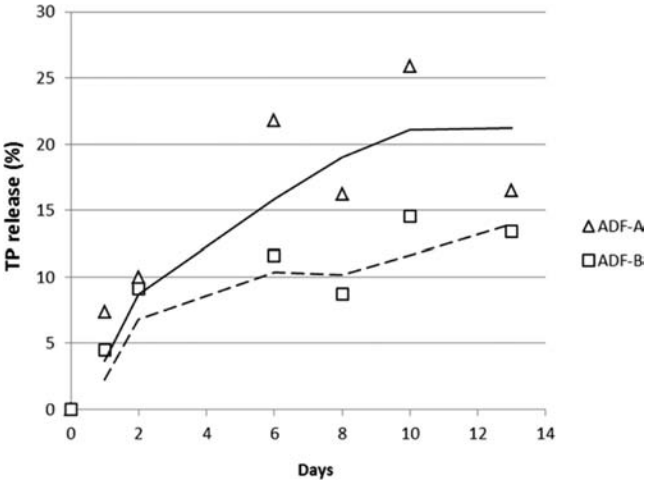

Figure 2. Profile of diffusion of TP (%) from ADF-A and ADF-B according to a 2 periods-moving average regression.

by periodic extrapolation. TP contents in MC-A and MC-B films at day 0 were similar (68.3 and 68.2 μg GAE/mg film for MC-A and MC-B, respectively), as standardized initial TP concentration in films. Overall, results show that TP availability in both MC-A and MC-B decreased continuously from day 0 to day 13 with TP values ranging from 68.3 to 57.0 μg GAE/mg for MC-A and from 68.2 to 59.0 μg GAE/mg for MC-B. These values represent diffusions of 21.2 and 14.0%, respectively, for MC-A and MC-B films after 14 days of storage. Between days 0 and 2, similar releases of TP were observed in both films ($p > 0.05$), showing a value of 61.5−62.0 μg GAE/mg of film at day 2. The diffusion curve (Figure 2) indicated TP releases at day 2 of 8.7 and 6.8% for MC-A and MC-B films, respectively. These data generated slopes of 4.4 and 3.4% TP/day, hence indicating a higher diffusion over this first subperiod. Between days 2 and 8, TP releases of ADF-A and ADF-B were significantly different ($p \leq 0.05$), showing releases of 19.0 and 10.2% for ADF-A and ADF-B, respectively, at day 8. These data generated slopes of 1.7 and 0.6% TP/day, suggesting a slower release during this second subperiod. Also, it can be observed that the slowdown of ADF-B diffusion was emphasized with a plateau observed from day 6, whereas a plateau was noted at day 10 for ADF-A. As a result, ADF-B films showed the lowest TP release during all storage, which may represent an advantage for long-term storage of food. From these results, it could be hypothesized that chemical interactions between antimicrobials and MC matrix could influence the TP release of antimicrobial volatiles, as suggested by previous studies.[26] Hence, the different

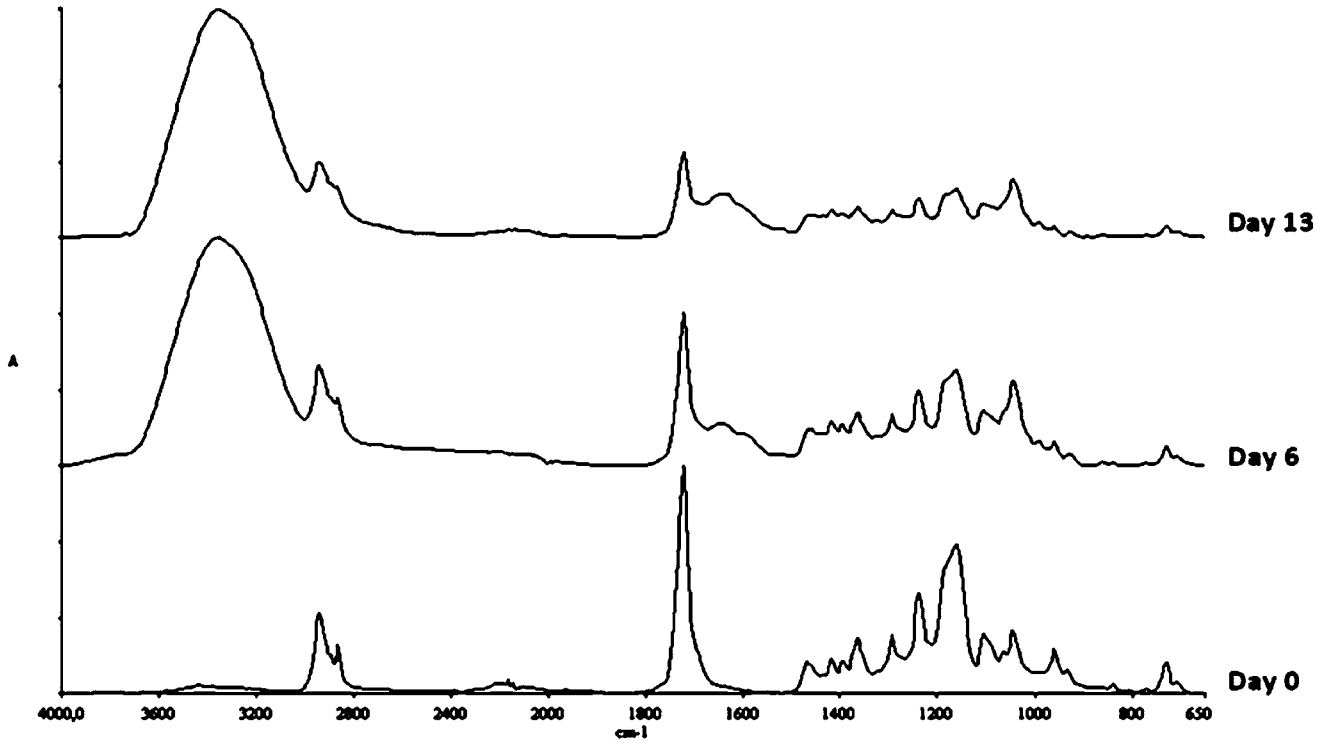

Figure 3. FTIR spectra of composite trilayer ADFs as related to time of storage at days 0, 6, and 13. Typical vibration bands of PCL-based external layers, related to water content in the films, are shown as a function of time.

Table 3. Characteristic IR Absorption Frequencies As Related to Figures 3 and 4 and Assignment of Typical Vibrations to the Chemical Groups of Film Components

related spectrum	wavenumber (cm^{-1})	vibration	functional group
Figure 3 (trilayer ADFs)	3600−3000	OH stretching	water
	2950−2850	C−H antisymmetric and symmetric stretching	$-CH_2$ and $-CH_3$ in aliphatic compounds
	1720	C═O stretching	−C═O in lactones
	1635	−OH bending	−OH in water
	1240	C—O—C antisymmetric stretching	−C—O—C in ethers and esters
	1180−1160	C—O stretching	−C—O in lactones
Figure 4, spectrum a (internal layer MC-control)	3600−3200	−OH stretching	−OH in alcohols/phenols[17]
	2960−2870	−C—H symmetric stretching	$-CH_2$ and $-CH_3$ in aliphatic compounds[17]
	1800−1600	−OH bending	−OH in water associated with MC[17,34]
	1500−1270	−C—H symmetric and asymmetric bending	degree of order in MC[34,35]
	1160−950	−C—O—C antisymmetric stretching and carbon ring	−C—O—C cellulose ethers and −C—CH from carbon rings in cyclic compounds[17,22]
Figure 4, spectrum b (rosemary extract)	3600−3200	−OH stretching	−OH in alcohols/phenols
	3100−2400	−OH stretching	−OH in carboxylic acid groups
	3100−3000	═CH stretching	═CH in aromatic and unsaturated hydrocarbons
	1690	−C═O stretching	−C═O in unsaturated ester and carboxylic acid
	1600 and 1516	aromatic ring stretching	aromatic compounds
	1256	C—O—C antisymmetric stretching	C—O—C in ester groups
Figure 4, spectra c and d (formulations A and B)	3600−3200	OH stretching (predominant in spectrum d)	−OH in alcohols/phenols
	3100−2850	−C—H symmetric stretching	−C—H in aliphatic and unsaturated hydrocarbons
	1670−1660	−C═O stretching	−C═O in unsaturated esters, aldehydes and ketones
	1600 and 1515	aromatic ring stretching	aromatic compounds
	1450−1250	−C—H bending and C−O−C stretching	terpenic compounds and esters from EOs
Figure 4, spectrum e (internal layer MC-B)	3600−3100	−OH stretching	−OH in aromatics/phenolics
	3100−2850	−C—H symmetric stretching	−C—H in aliphatic and unsaturated hydrocarbons
	1600 and 1515	aromatic ring stretching	aromatic compounds
	1265	C—O—C antisymmetric stretching	C—O—C in ester groups

percentages obtained for ADF-A and -B could be related to the chemical nature and volatility of major phenolic components in formulations A and B during the diffusion process. Chemical interactions between bioactive molecules and film components, and the resulting diffusion of volatiles, are described below in FTIR analysis.

FTIR Analysis of ADFs. *Analysis of ADFs as a Function of Time.* FTIR spectra of ADFs (composite trilayer films) at different days of storage, with spectra corresponding to days 0, 6 and 13, are presented in Figure 3. As shown in Table 3, the absorption sharp peaks of spectrum at day 0 (2950−2850, 1720, and 1180−1160 cm^{-1}) are mainly assigned to IR vibrations of PCL (external layer of ADFs). The comparison of these three spectra allowed characterization of the hydration of ADFs during storage, by progressive increase of peak intensity related to water absorption and by resulting decrease of intensity related to PCL functional groups. Indeed, typical bands from water such as O−H stretching and O−H bending appeared during storage, as indicated by spectra at days 6 and 13. Meanwhile, this hydration resulted in a decrease of intensity of all main peaks attributed to PCL. These results supported that water detection would come from hydration of internal water-soluble MC-based film, whereas PCL is strongly hydrophobic. Similar observations suggesting a reduction of signal from hydrophobic compounds to the detriment of a hydration process were already reported by Salmieri and Lacroix.[24]

Analysis of the Composition of Internal MC Layer. FTIR spectra of (a) MC-control, (b) rosemary extract powder, (c) formulation A, (d) formulation B, and (e) MC-B, that is, MC matrix containing formulation B, are presented in Figure 4. It should be noted that the spectrum of MC-A is not presented because it was identical to that of MC-B (totally overlapped spectra). Also, the FTIR spectrum of liquid smoke was not used in FTIR comparison due to its very weak signal as compared to other antimicrobial compounds, implying totally masked absorption bands in resulting spectrum e.

Spectra c and d are typical FTIR profiles of EOs, with vibration bands mainly attributable to phenolic and terpenic groups. However, some differences can be noted between spectra c (formulation A) and d (formulation B), due to their respective major components. Indeed, a strong band related to O−H stretching can be observed in spectrum d, suggesting that formulation B is composed of a major part of phenolic compounds as compared to formulation A that would contain more hydrocarbon terpenic compounds. Spectrum e represents the FTIR profile of MC-B, hence containing typical absorption bands of MC-matrix and antimicrobial compounds such as

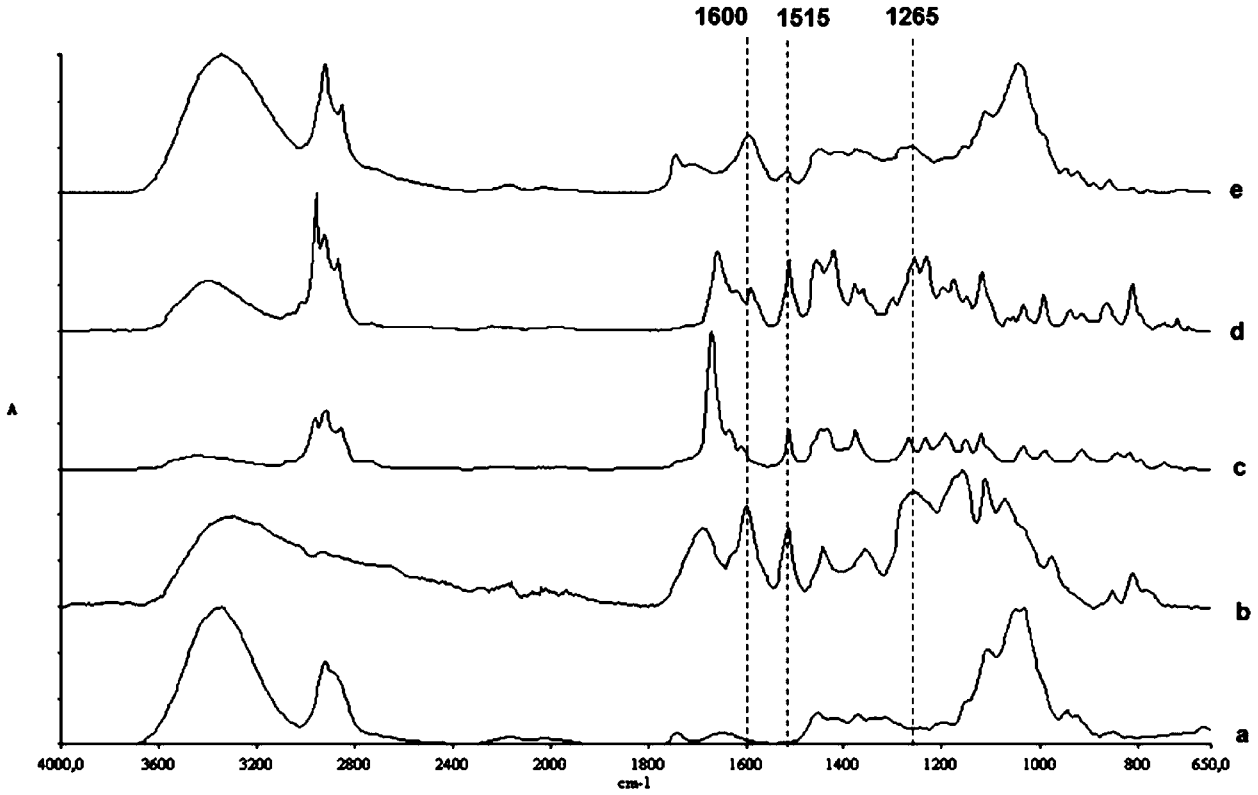

Figure 4. FTIR spectra related to the composition of MC-control (a), rosemary extract (b), formulation A (c), formulation B (d), and MC-B (e). Bands at 1600, 1515, and 1265 cm^{-1} are related to aromatic and ester groups from antimicrobial compounds (spectra b–d) and are exploitable in ADF-B (spectrum e) for further quantification of the TP release of bioactive ADFs.

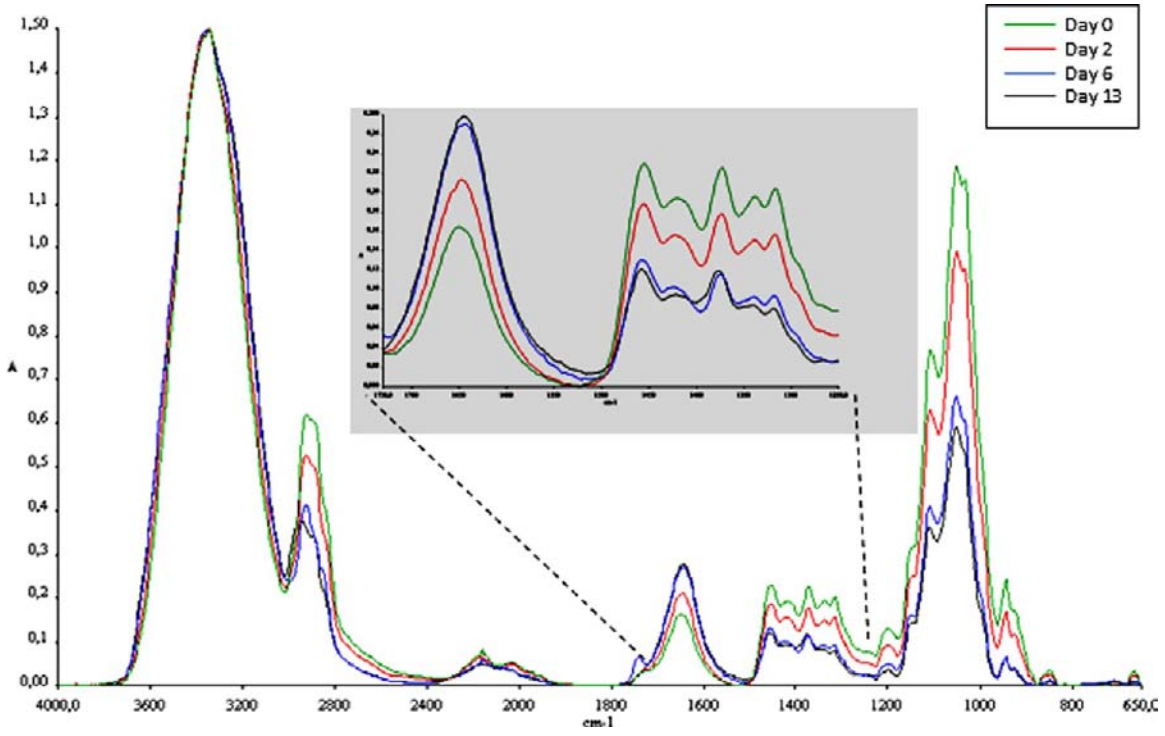

Figure 5. FTIR spectra of MC-control internal films as related to storage time, with focus on the fingerprint region (1250–1730 cm^{-1}). Color of spectra indicates the day of analysis: green (day 0), red (day 2), blue (day 6), and black (day 13).

rosmarinic acid and formulation B. Some differences can be highlighted in the whole infrared (IR) region after incorporation of formulation B in the MC matrix. Indeed, as referred to spectrum a, a broader band is observed in spectrum e at 3600–3100 cm^{-1}, related to typical O–H vibrations of aromatic/phenolic compounds in formulation B. In addition, a stronger

dx.doi.org/10.1021/jf304439s | J. Agric. Food Chem. 2013, 61, 811–821

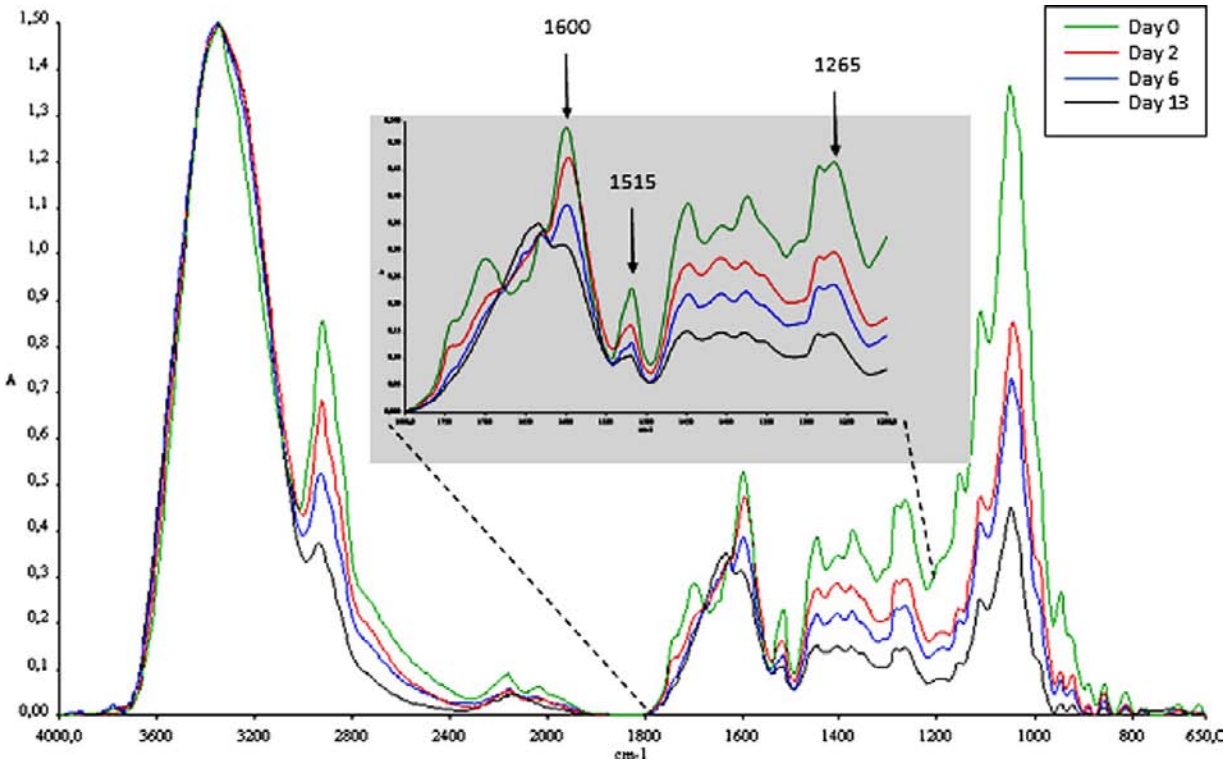

Figure 6. FTIR spectra of MC-B internal films as related to storage time, with focus on the fingerprint region (1200−1800 cm^{-1}). Color of spectra indicates the day of analysis: green (day 0), red (day 2), blue (day 6), and black (day 13). Note that FTIR spectra of MC-A films presented exactly the same peaks that evolved in a very similar way.

Table 4. Percentage of Peak Height of Typical IR Bands at 1600, 1515, and 1265 cm^{-1} for Semiquantitative Estimation of the Diffusion of Antimicrobial Compounds from MC-A and MC-B Films during Storage

		peak height[a]			percentage of peak height[b]		
film	day	1600 cm^{-1}	1515 cm^{-1}	1265 cm^{-1}	1600 cm^{-1}	1515 cm^{-1}	1265 cm^{-1}
MC-A	0	0.4609	0.1838	0.2832	100.00	100.00	100.00
	1	0.4073	0.1506	0.1901	88.37	81.94	67.13
	2	0.3986	0.1503	0.1932	86.48	81.77	68.22
	6	0.2866	0.1106	0.0860	62.18	60.17	30.37
	13	0.2651	0.1022	0.0652	57.52	55.60	23.02
MC-B	0	0.4845	0.2294	0.3825	100.00	100.00	100.00
	1	0.4248	0.1705	0.2430	87.68	74.32	63.53
	2	0.3923	0.1597	0.2154	80.97	69.62	56.31
	6	0.3402	0.1279	0.1549	70.22	55.75	40.50
	13	0.2636	0.1033	0.0629	54.41	45.03	16.44

[a]Peak heights at 1600, 1515, and 1265 cm^{-1} are associated with semiquantitative estimation of quantities of antimicrobial compounds according to their chemical nature. Therefore, measurements of decreasing values at 1600 and 1515 cm^{-1} were used to evaluate the diffusion of aromatic volatile compounds, whereas measurements at 1265 cm^{-1} were used to estimate the diffusion of ester volatile compounds. [b]Percentage of relative peak (%) = (peak height/peak height at day 0) × 100.

and asymmetric band occurs at 3100−2850 cm^{-1}, underlying the presence of aliphatic and unsaturated hydrocarbons related to terpenoid components. Clearer changes in spectrum e can be noted with the appearance of vibrational bands associated with antimicrobials and involving ring stretching modes of aromatic groups at 1600 and 1515 cm^{-1} and C−O−C antisymmetric stretch mode of esters at 1265 cm^{-1}.

Hence, Figure 4 shows that the evolution of the spectra from spectra a to e was consistent as related to the chemical nature of each film component (a−d) and the additive effect of their strong peaks in the whole MC-A or -B film formulation.

TP Release by FTIR Analysis. *Identification of Bands Related to Diffused Antimicrobials.* The evolution of FTIR spectra of MC-control and MC-B during storage, at days 0, 2, 6, and 13, is presented in Figures 5 and 6. Note that FTIR spectra of MC-A-based films are not shown because they presented similar evolving peaks as those of MC-B-based films. This analysis focused on the fingerprint region (1800−1200 cm^{-1}) of MC internal layer (i) to take into consideration the evolution of the bands ascribed to the hydration of MC matrix (Figure 5) and also (ii) to evaluate the diffusion of antimicrobial volatile compounds (Figure 6). Spectra were normalized by setting O−H stretching bands up to 1.5 absorbance units (AU) to subtract

dx.doi.org/10.1021/jf304439s | J. Agric. Food Chem. 2013, 61, 811−821

water absorption in MC matrix. Moreover, the analysis of fingerprint region allowed differentiating the peaks that were associated with antimicrobial compounds. In general, spectra in Figures 5 and 6 present the same evolution in higher frequencies (4000−2400 cm^{-1}). For each sample (MC-control and MC-B), the O−H stretching vibration at 3600−3200 cm^{-1} broadened during storage (days 0−13), suggesting hydration of MC matrix, which is in agreement with results obtained for ADFs (Figure 3), and similar observations have already been reported by Le Tien et al.[27] for cellulose-based films. In the meantime, this band broadening due to hydration was also accompanied by a reduced intensity of C−H stretching vibrations at 2950−2850 cm^{-1} (hydrophobic groups), as described above (Figure 3). The fingerprint IR region in Figure 5 shows that the bound water vibration of MC-control at 1650 cm^{-1} increased during storage (relatively to hydration effect), whereas its vibration modes related to degree of order decreased at 1500−1270 cm^{-1}, possibly due to a reduced resonance of methylated groups in MC, as reported by Khan et al.[17]

Figure 6 shows the evolution of FTIR spectra of MC-B internal films during storage. In comparison with Figure 5 (MC-control), the fingerprint region of Figure 6 indicates the appearance of three typical peaks associated with antimicrobial formulation B such as ring stretching modes of aromatic groups at 1600 and 1515 cm^{-1} and C−O−C antisymmetric stretch mode of esters at 1265 cm^{-1}, which is congruent with observations in Figure 3e. It can also be observed that the intensity of these three peaks decreased during storage, thereby indicating a diminution of antimicrobial contents in MC matrix. This profile suggests a diffusion of antimicrobial volatiles toward external environment (headspace), which is in accordance with results obtained for TP quantification (Table 2 and Figure 2).

Semiquantification of IR Bands. To correlate FTIR analysis of the bands related to diffused antimicrobials with TP results (Table 2), the peak heights (absorbance) of IR bands at 1600, 1515, and 1265 cm^{-1} of MC-A and MC-B films, and their relative percentage during storage, were measured and are presented in Table 4. Results show that the percentage of IR peaks related to antimicrobial volatiles decreased progressively over time, suggesting a slow diffusion of volatiles from the films to packaging headspace. If considering proportionality of peak height with availability of compounds in the film, the evolution of percentage of peak height in MC-A at 1600 cm^{-1} (aromatic compounds) is analogous to MC-B, with variations from 100 to 54−58% between days 0 and 13. In comparison, the progression of peak heights at 1515 and 1265 cm^{-1} seems to be less analogous between the two types of films, with reductions to 45−56% at 1515 cm^{-1} and to 16−23% at 1265 cm^{-1}, over the same period. These observations demonstrate that the diffusion of antimicrobial compounds during time storage could be monitored by FTIR quantification of related bands.

Correlation between FTIR Analysis and TP Measurements. Correlations between TP concentrations and FTIR peak heights were investigated by a simple type of regression to verify linear correlations between the two methods. Calculations allowed concluding it was possible to establish a satisfying correlation (>0.90) between TP measurements and the absorbance of FTIR peaks at 1600 cm^{-1} for both antimicrobial films ADF-A and -B. Linear correlation of IR absorbance at 1600 cm^{-1} versus TP concentration (μg GAE/mg) is presented in Figure 7 and shows that (i) plotting of ADF-A data resulted in a linear equation, $y = 0.0063x - 0.0116$

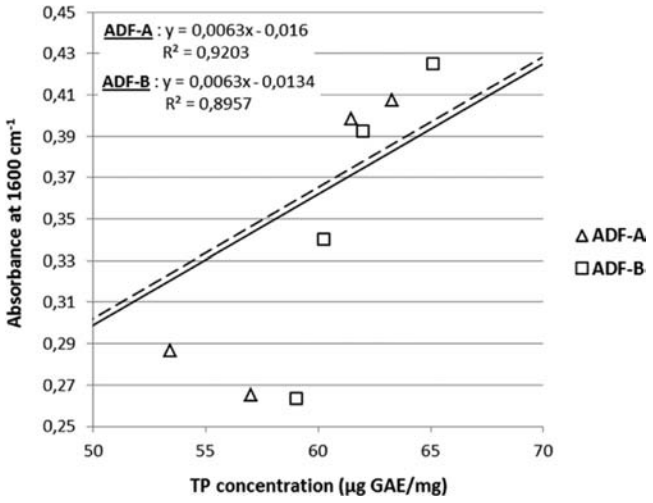

Figure 7. Linear correlation between FTIR absorbance at 1600 cm^{-1} of ADF-A and ADF-B and their availability of TP concentration (μg GAE/mg) determined by spectrophotometry, as deduced from data obtained in Tables 2 and 4.

($R^2 = 0.92$), and (ii) plotting of ADF-B data generated the equation $y = 0.0063x - 0.0134$ ($R^2 = 0.90$). Consequently, semiquantitative estimation of peak absorbance at 1600 cm^{-1} (group of aromatic volatiles including phenolic compounds) can offer an accurate, rapid, and nondestructive analytical method to evaluate the TP release toward the package headspace over storage time.

SEM Analysis. SEM was carried out for extensive morphological inspection of cross section in MC internal layer and to evaluate the effect of NCC filling and antimicrobial incorporation on the internal structure of MC matrix. The effect of NCC alone (without antimicrobials) was justified due to the fact that antimicrobials were preliminarily dispersed in NCC suspension before their incorporation in MC matrix for the preparation of ADFs. SEM micrographs of three different internal MC layers from ADFs containing (i) no NCC and no antimicrobials (A-1; A-2), (ii) NCC with no antimicrobials (MC-control) (B-1; B-2), and (iii) NCC with formulation B (MC-B) (C-1; C-2) are presented in Figure 8. Two magnifications (600× and 10000×) were used to evaluate the cross section of films. Parts A-1 and A-2 represent a nonfibrillar structure that tends to adopt a globular organization (smooth structure with globular cavities). The addition of NCC in MC matrix clearly affected the structure of films. Indeed, as shown in parts B-1 and B-2, the cross section of MC-control appears to be rougher and denser, implying the filling of NCC into the polymer bulk while maintaining some more dispersed globular heterogeneous areas. Analogous SEM images of NCC into polysaccharide matrices were reported by other studies.[17,28] On the other hand, the addition of bioactive agents (formulation B), as described in C-1 and C-2, results in a very homogeneous (denser structure) and more granular cross section (less smooth with up and down serration shape as compared to other samples) as compared to MC-control. This finer, homogeneous, and more regular order can be attributed to the presence of bioactive agents interspersed into the polymer network. In particular, these observations could suggest that

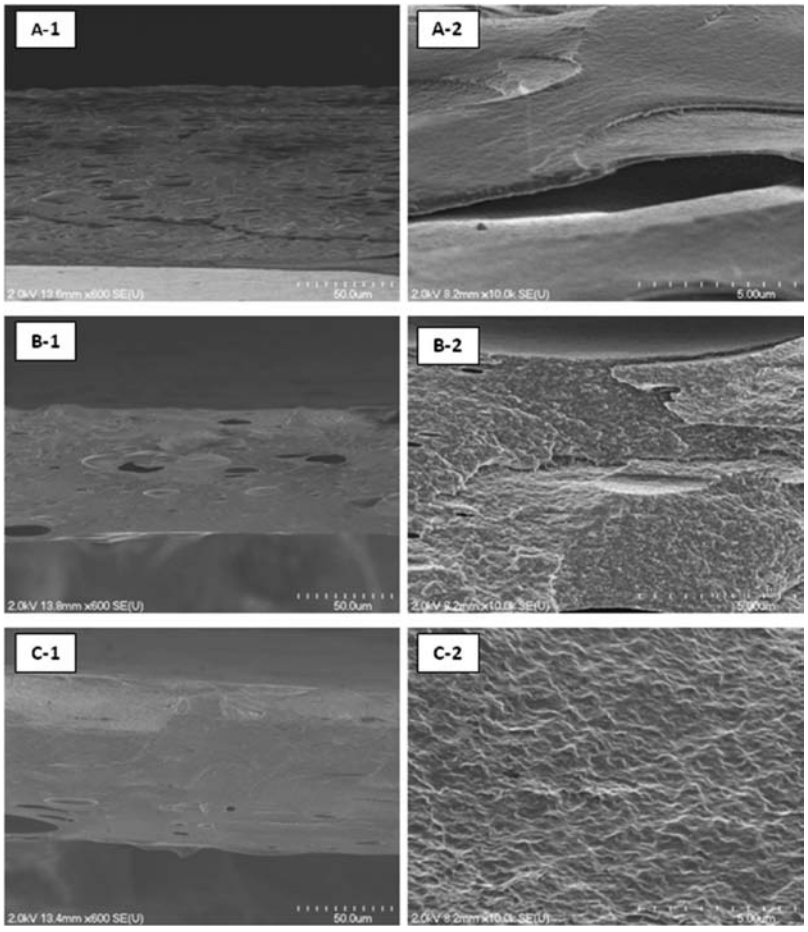

Figure 8. Cross-sectional SEM micrographs of internal bioactive MC layers from ADFs: (A-1) control film without NCC at magnification 600×; (A-2) control film without NCC at magnification 10000×; (B-1) control film at magnification 600×; (B-2) control film at magnification 10000×; (C-1) MC layer containing formulation B at magnification 600×; (C-2) MC layer containing formulation B at magnification 10000×.

Table 5. Colorimetric Parameters of ADFs as a Function of Storage Time and Antimicrobial Formulations[a]

	film	day 0	day 6	day 13
L^*	ADF-control	92.23 ± 0.21 b,A	92.10 ± 0.26 b,A	92.43 ± 0.59 c,A
	ADF-A	69.60 ± 2.48 a,B	60.80 ± 3.73 a,A	60.20 ± 1.34 a,A
	ADF-B	71.00 ± 1.15 a,B	66.13 ± 4.56 a,AB	63.10 ± 1.65 b,A
h°	ADF-control	123.42 ± 4.61 b,A	120.4 ± 3.90 b,A	122.19 ± 6.59 b,A
	ADF-A	87.72 ± 1.28 a,B	83.99 ± 1.88 a,A	84.37 ± 0.58 a,A
	ADF-B	88.84 ± 0.80 a,A	87.06 ± 2.25 a,A	86.02 ± 0.89 a,A

[a]Means followed by the same lower case letter in each column for each property are not significantly different at the 5% level. Means followed by the same upper case letter in each row are not significantly different at the 5% level. N/A, nonapplicable.

NCC aggregates inserted into MC network have kept much of their original physical properties in the presence of bioactive compounds, therefore increasing the tridimensional morphology of MC layer. Similar morphological trends were reported by Khan et al. and Salmieri and Lacroix.[17,24]

Physicochemical Properties of Films. *Colorimetry of Films.* Colorimetric measurements of ADFs were carried out using the CIELAB system to evaluate the effect of the presence of antimicrobial formulations A and B on the lightness (L^*) and hue angle of films during storage.

Evolution of the Lightness (L^*). Results presented in Table 5 clearly show that ADF-control exposes a stable lightness over time ($p > 0.05$) that approaches absolute white ($L^* = 92\%$), whereas antimicrobial films (ADF-A and ADF-B) display a lower lightness (L^* between 60 and 71%) throughout storage due to the presence of colored antimicrobial extracts encapsulated in the film matrix (Table 5). Moreover, as opposed to ADF-control, antimicrobial films present lightness variations over storage. A significant decrease of L^* values ($p \leq 0.05$) was observed from 70 to 60 for ADF-A and from 71 to 63 for ADF-B, indicating a significant darkening of these films. Hence, the decrease of the L^* values of ADFs during storage could be due to the hydration of ADFs as well as the autoxidation of encapsulated antimicrobial extracts (in particular phenolic compounds), as already observed by numerous studies.[2,29]

Evolution of the Hue Angle. A stability of the hue values was observed in ADF-control and ADF-B, showing no

dx.doi.org/10.1021/jf304439s | J. Agric. Food Chem. 2013, 61, 811−821

significant difference ($p > 0.05$) over time. Indeed, results indicate that the hue of ADF-control was maintained in the yellow-green area (hue = 120−123°) and that of ADF-B was maintained in the yellow area (hue = 86−89°). In comparison, ADF-A generated a significant decrease ($p \leq 0.05$) of the hue from 88 to 84°, equivalent to a slightly turning-red yellowness of these films, probably due to the chemical nature of antimicrobial compounds that were affected by oxidation in formulation A. Hence, the hue values of ADF-A and ADF-B combined with their lower L^* values imply a slightly browner color of these films as compared to ADF-control, due to the presence of antimicrobial extracts encapsulated in the film and their oxidation over time, as observed for L^* measurements. Furthermore, due to a significant decrease of hue value ($p \leq 0.05$) of ADF-A between days 0 and 6, it could be assessed that the composition of formulation A tended to generate more browning reactions by oxidation, as compared to ADF-B. This phenomenon is supported by a significantly lower value of L^* ($p \leq 0.05$) for ADF-A at day 13 (60 for ADF-A and 63 for ADF-B). With regard to combined results from L^* and hue angle measurements, it can be noted that ADF-A seems to be more sensitive than ADF-B in color changes because it demonstrated a more rapid significant variation ($p \leq 0.05$) of lightness and hue from day 0 to day 6 (L^* from 70 to 60 and hue from 88 to 84°). This propensity for a brown-turning color behavior of ADF-A could be explained by a lower antioxidant activity of antimicrobial components in formulation A, which is congruent with results reported by other studies.[30,31]

Mechanical Properties. *Evaluation of the Tensile Strength (TS).* TS values of ADFs as a function of storage time are presented in Table 6. TS is the ultimate strength (or maximum stress) of a material subjected to tensile loading. Results show that all ADFs possessed similar resistance ($p > 0.05$) at day 0, with TS values between 20 and 24 MPa. The TS of ADF-control did not vary over time ($p > 0.05$), with values ranging from 20.3 to 18.7 MPa between days 0 and 13. On the other hand, the TS of antimicrobial ADFs was reduced significantly ($p \leq 0.05$) during storage. Indeed, the TS values decreased from 23.7 to 7.8 MPa for ADF-A (reduction of 67%) and from 24.0 to 17.3 MPa for ADF-B (reduction of 28%) after 14 days of storage. However, at day 13, results show no significant difference ($p > 0.05$) between ADF-control and ADF-B with similar TS values of 17.3−18.7 MPa, whereas the TS of ADF-A was significantly lower ($p \leq 0.05$) at 7.8 MPa. Hence, these observations imply that ADF-A was significantly less resistant to tensile stress than ADF-control and ADF-B ($p \leq 0.05$) over storage. These behaviors could be explained by the chemical nature of antimicrobials that interacted differently according to the type of antimicrobial formulation and in combination with the hydration of films over storage, as described below for TM interpretation. Moreover, it is well-known that the incorporation of EOs into a continuous polymeric matrix tends to decrease its mechanical resistance to fracture because of the structural discontinuities caused by the oil-dispersed phase.[24,32]

Table 6. Effect of Antimicrobial Formulation on the Tensile Strength of ADFs during Storage

	tensile strength[a] (MPa)		
film	day 0	day 6	day 13
ADF-control	20.3 ± 4.9 a,A	19.1 ± 2.7 a,A	18.7 ± 3.7 b,A
ADF-A	23.7 ± 2.7 a,C	18.0 ± 2.7 a,B	7.8 ± 0.7 a,A
ADF-B	24.0 ± 3.4 a,B	20.4 ± 1.4 a,A	17.3 ± 2.0 b,A

[a]Means followed by the same lower case letter in each column are not significantly different at the 5% level. Means followed by the same upper case letter in each row are not significantly different at the 5% level.

Evaluation of the Tensile Modulus (TM). TM values of ADFs as a function of storage time are presented in Table 7. TM (or Young's modulus) is a tangent modulus of elasticity of a material subjected to tensile loading and is expressed by the ratio of stress to elastic strain in tension. A high TM means that the material is rigid. Results show that ADF-control and ADF-B possessed similar viscoelastic properties ($p > 0.05$) at day 0, with respective TM values of 218 and 210 MPa. Otherwise, the TM value of ADF-A was significantly lower ($p \leq 0.05$) than those of ADF-control and ADF-B at day 0, with a value of 175 MPa, suggesting that the incorporation of formulation A improved the viscoelasticity of ADFs due to the chemical nature of its components and their possible plasticizing effect on MC-based internal matrix. Similar observations were reported by Salmieri and Lacroix[24] for investigation on mechanical properties of films containing different EOs. For each ADF formulation, TM values decreased significantly ($p \leq 0.05$) over storage, from 218 to 111 MPa for ADF-control (reduction of 49%), from 175 to 89 MPa for ADF-A (reduction of 49%), and from 210 to 85 MPa for ADF-B (reduction of 59%). Such TM reductions could be closely related to the hydration of ADFs during time, thereby enhancing their elasticity based on an alteration of hydrogen bonding in MC network.[33] These data are in accordance with hydration phenomenon in ADFs characterized by FTIR spectra from Figure 3 and therefore support these mechanical changes. Additionally, ADF-control tended to be more rigid as compared to antimicrobial films during storage, with higher TM values. It is proposed that the hydration of MC matrix over time could promote the plasticizing action of antimicrobial compounds. Similar results have already been reported by Salmieri and Lacroix[24] concerning the combined effect of EO incorporation and dehydrating treatment of polysaccharide-based films.

As a result, these mechanical measurements allowed characterizing ADF-control as a resistant but less elastic

Table 7. Effect of Antimicrobial Formulation on the Tensile Modulus of ADFs during Storage

	tensile modulus[a] (MPa)		
film	day 0	day 6	day 13
ADF-control	218.3 ± 27.2 b,B	124.1 ± 14.6 b,A	110.6 ± 3.8 b,A
ADF-A	175.2 ± 26.6 a,B	106.0 ± 10 a,A	89.40 ± 10.5 a,A
ADF-B	209.6 ± 20.2 b,C	124.7 ± 22.7 b,B	84.8 ± 9.6 a,A

[a]Means followed by the same lower case letter in each column are not significantly different at the 5% level. Means followed by the same upper case letter in each row are not significantly different at the 5% level.

material over time. In contrast, ADF-A was determined as an elastic but less resistant material over time. Meanwhile, ADF-B could be ascribed (i) to a more resistant long-term material compared to ADF-A and also (ii) to a more elastic material compared to ADF-control, hence gathering higher combined mechanical properties (TM and TS) over storage.

In summary, trilayer ADFs developed in this study showed very satisfactory physicochemical and in vitro antimicrobial properties and could further be explored in food applications to prevent pathogenic contamination during storage of ready-to-eat foods. FTIR analysis allowed characterization of the molecular interactions occurring after incorporation of antimicrobials, and SEM observations provided a typical morphological structure of the films due to the filling of the NCC−antimicrobials emulsion into polymer bulk. Moreover, ADFs allowed a slow controlled release of the antimicrobial compounds during storage. This study has also demonstrated that it is possible to follow the TP release of the antimicrobial compounds by FTIR with satisfying correlations (>90%) compared to standard method. Addition of antimicrobials increased the elasticity of the films, and ADF-B was determined as more resistant than ADF-A. Moreover, the incorporation of antimicrobials in ADFs promoted only slight variations of their color. To complete these investigations, further tests are to be carried out on the sensorial quality of the packaged vegetables treated with ADFs during storage and also in situ microbiological analyses during storage using vegetables inoculated by pathogenic foodborne bacteria.

AUTHOR INFORMATION

Corresponding Author

*Phone: +1 (450) 687-5010. Fax: +1 (450) 686-5501. E-mail: monique.lacroix@iaf.inrs.ca.

Funding

The Québec Ministry of Agriculture, Fisheries and Food is particularly acknowledged for their financial support through the PSIA program (Programme de Soutien à l'Innovation en Agroalimentaire).

Notes

The authors declare no competing financial interest.

ACKNOWLEDGMENTS

We are grateful to FPInnovations (Pointe-Claire, Quebec, Canada) for providing NCC generously. We are thankful to P. L. Thomas & Co. Inc., Kerry Ingredients and Flavours, and BSA Food Ingredients s.e.c./l.p. for graciously providing natural antimicrobials. We highly appreciated the assistance of Line Mongeon, Technician of Biomedical Engineering Department and Facility Electron Microscopy Research (FEMR) at McGill University, for SEM support. Finally, we thank Winpak Division Ltd. for providing packaging material.

REFERENCES

(1) Matthews, B.; Mangalasary, S.; Darby, D.; Cooksey, K. *Packag. Technol. Sci.* **2010**, *23*, 267−273.
(2) Devlieghere, F.; Vermeiren, L.; Debevere, J. *Int. Dairy J.* **2004**, *14*, 273−285.
(3) Dehkharghanian, M.; Salmieri, S.; Lacroix, M.; Vijayalakshmi, M. A. *Dairy Sci. Technol.* **2009**, *89*, 485−499.
(4) Han, J.; Guenier, A. S.; Salmieri, S.; Lacroix, M. *J. Agric. Food Chem.* **2008**, *56*, 2525−2535.
(5) Caillet, S.; Salmiéri, S.; Lacroix, M. *Food Chem.* **2006**, *95*, 1−8.
(6) Conner, D. E.; Beuchat, L. R. *J. Food Sci.* **1984**, *49*, 429−434.
(7) Oussalah, M.; Caillet, S.; Salmieri, S.; Saucier, L.; Lacroix, M. *J. Agric. Food Chem.* **2004**, *52*, 5598−5605.
(8) Conner, D. E., In *Antimicrobials in Foods*, 2nd ed.; Davidson, P., Branen, A. L., Eds.; Dekker: New York, 1993; pp 441−468.
(9) Oussalah, M.; Caillet, S.; Saucier, L.; Lacroix, M. *Food Control.* **2007**, *18*, 414−420.
(10) Oussalah, M.; Caillet, S.; Salmiéri, S.; Saucier, L.; Lacroix, M. *J. Food Prot.* **2006**, *69*, 2364−2369.
(11) Takala, P. N.; Vu, K. D.; Salmieri, S.; Lacroix, M. *J. Food Prot.* **2011**, *74*, 1065−1069.
(12) Vu, K. D.; Hollingsworth, R. G.; Leroux, E.; Salmieri, S.; Lacroix, M. *Food Res. Int.* **2011**, *44*, 198−203.
(13) Yoshii, F.; Darwis, D.; Mitomo, H.; Keizo, M. *Radiat. Phys. Chem.* **2000**, *57*, 417−420.
(14) Goupil, D. In *Biomaterials Science*; Ratner, B. D., Hoffman, A. S., Schoen, F. J., Lemons, J. E., Eds.; Academic Press: New York, 1996; pp 356−360.
(15) Kohn, J.; Langer, R. In *Biomaterials Science*; Ratner, B. D., Hoffman, A. S., Schoen, F. J., Lemons, J. E., Eds.; Academic Press: New York, 1996; pp 64−72.
(16) Lewis, O. G.; Fabisial, W. In *Kirk−Othmer Encyclopedia of Chemical Technology*, 4th ed.; Wiley: New York, 1997.
(17) Khan, R. A.; Salmieri, S.; Dussault, D.; Uribe-Calderon, J.; Kamal, M. R.; Safrany, A.; Lacroix, M. *J. Agric. Food Chem.* **2010**, *58*, 7878−7885.
(18) Favier, V.; Chanzy, H.; Cavaillé, J. Y. *Macromolecules* **1995**, *28*, 6365−6367.
(19) Klemm, D.; Schumann, D.; Kramer, F.; Hebler, N.; Koth, D.; Sultanova, B. *Macromol. Symp.* **2009**, *280*, 60−71.
(20) Azeredo, H. M. C.; Mattoso, L. H. C.; Avena-Bustillos, R. J.; Filho, G. C.; Munford, M. L.; Wood, D.; McHugh, T. H. *J. Food Sci.* **2010**, *75*, N1−N7.
(21) Klemm, D.; Schumann, D.; Kramer, F.; Heßler, N.; Hornung, M.; Schmauder, H. P.; Marsch, S. *Adv. Polym. Sci.* **2006**, 49−96.
(22) Sharmin, N.; Khan, R.; Salmieri, S.; Dussault, D.; Lacroix, M. *J. Polym. Environ.* **2012**, 1−8.
(23) Rojas-Grau, M. A.; Avena-Bustillos, R. J.; Friedman, M.; Henika, P. R.; Martin-Belloso, O.; McHugh, T. H. *J. Agric. Food Chem.* **2006**, *54*, 9262−9267.
(24) Salmieri, S.; Lacroix, M. *J. Agric. Food Chem.* **2006**, *54*, 10205−10214.
(25) Jin, T.; Zhang, H. *J. Food Sci.* **2008**, *73*, M127−M134.
(26) López, P.; Sánchez, C.; Batlle, R.; Nerín, C. *J. Agric. Food Chem.* **2007**, *55*, 8814−8824.
(27) Le Tien, C.; Letendre, M.; Ispas-Szabo, P.; Mateescu, M. A.; Delmas-Patterson, G.; Yu, H. L.; Lacroix, M. *J. Agric. Food Chem.* **2000**, *48*, 5566−5575.
(28) Azeredo, H. M. C.; Mattoso, L. H. C.; Wood, D.; Williams, T. G.; Avena-Bustillos, R. J.; McHugh, T. H. *J. Food Sci.* **2009**, *74*, N31−N35.
(29) Donhower, I. G.; Fennema, O. *J. Food Process. Preserv.* **1993**, *17*, 247−257.
(30) Bagamboula, C. F.; Uyttendaele, M.; Debevere, J. *Food Microbiol.* **2004**, *21*, 33−42.
(31) Chisari, M.; Todaro, A.; Barbagallo, R. N.; Spagna, G. *Food Chem.* **2010**, *119*, 1502−1506.
(32) Sanchez-Gonzalez, L.; Vargas, M.; Gonzalez-Martinez, C.; Chiralt, A.; Chafer, M. *Food Eng. Rev.* **2011**, *3*, 1−16.
(33) Zsivánovits, G.; Marudova, M.; Ring, S. *Colloid Polym. Sci.* **2005**, *284*, 301−308.
(34) Velasquez, G.; Herrera-Gomez, A.; Martin-Polo, M. O. *J. Food Eng.* **2003**, *59*, 79−84.
(35) Filho, G. R.; Assunçao, R. M. N.; Vieira, J. G.; Meireles, C. S.; Cerquiera, D. A.; Barud, H. S.; Ribeiro, S. J. L.; Messaddeq, Y. *Polym. Degrad. Stab.* **2007**, *92*, 205−210.